Variability in Isolated Convective Activity between Louisville, Kentucky and Nearby Rural Locations

Jason Naylor*
Department of Geography and Geosciences, University of Louisville, Louisville, KY

Aaron D. Kennedy
Department of Atmospheric Sciences, University of North Dakota, Grand Forks, ND

Submitted to Earth Interactions

Corresponding Author Address: Jason Naylor, Department of Geography and Geosciences, University of Louisville, Louisville, KY, 40292. Email: jason.naylor@louisville.edu

Abstract

This study analyzes the frequency of strong, isolated convective cells in the vicinity of Louisville, Kentucky. Data from the Severe Weather Data Inventory (SWDI) are used to compare the frequency of convective activity over Louisville to the observed frequency at nearby rural locations from 2003–2019. The results show that Louisville experiences significantly more isolated convective activity compared to the rural locations. The difference in convective activity between Louisville and the rural locations is strongest during summer, with peak differences occurring between May and August. Compared to the rural locations, Louisville experiences more isolated convective activity in the afternoon and early evening, but less activity after midnight and into the early morning. Isolated convective events over Louisville are most likely during quiescent synoptic conditions, while rural events are more likely during active synoptic patterns.

To determine if these differences can be attributed primarily to urban effects, two additional cities are shown for comparison—Nashville, Tennessee and Cincinnati, Ohio. Both Nashville and Cincinnati experience more isolated convective activity than all five of their nearby rural comparison areas, but the results for both are statistically significant at four of the five rural locations. In addition, the analysis of Cincinnati includes a sixth comparison site that overlaps the urbanized area of Columbus, Ohio. For that location, differences in convective activity are not statistically significant.

1. Introduction

Numerous studies have found that precipitation patterns can be influenced by large urban areas. One of the first projects to study this effect was the Metropolitan Meteorological Experiment (METROMEX; e.g., Changnon et al. 1971; Huff and Changnon 1973; Changnon et al. 1977), which found evidence of precipitation enhancement downwind of St. Louis, Missouri. Since METROMEX, numerous subsequent studies have focused on other metropolitan areas. There is general agreement amongst these studies that urban areas can modify precipitation patterns, but results have differed regarding the type of modification, magnitude of the signal, and underlying physical mechanism(s) responsible for alterations to precipitation distributions around these areas.

While St. Louis, Missouri was the primary focus of many pioneering studies on urban-induced precipitation variations, Atlanta, Georgia has been the most frequent focus of modern studies (e.g., Dixon and Mote 2003; Mote et al. 2007; Shem and Shepherd 2009; Bentley et al. 2012; Haberlie et al. 2015). Although these studies have shown that Atlanta experiences more warm season convective events than surrounding rural regions, the results from one city should not necessarily be extrapolated to other large cities. For example, Huff and Changnon (1973) found evidence of urban-induced precipitation enhancement in six of eight cities studied, but there was substantial variability regarding magnitude, location, and even timing of the enhancement amongst those cities. Shepherd et al. (2002) found evidence of downwind precipitation enhancement in five different U.S. cities, however the magnitude of those anomalies (relative to precipitation amounts in the upwind area) varied from 15–51%. Furthermore, Ganeshan et al. (2013) determined that the urban influence on precipitation patterns varies by geography, with inland cities experiencing an increase in nocturnal convection and coastal cities experiencing an increase in afternoon convection. Recently, Liu and Niyogi (2019) performed a meta-analysis of previous studies on

urban-induced precipitation modification. They found that the most commonly reported signal was precipitation enhancement 20–50 km downwind of the urban center.

There is also some disagreement as to the exact physical mechanism responsible for urban-induced precipitation changes. While it has been suggested that surface roughness gradients (e.g., Hjelmfelt 1982; Thielen et al. 2000), urban aerosols (e.g., Jin et al. 2005; van den Heever and Cotton 2007; Stallins et al. 2013; Ochoa et al. 2015), and urban moisture availability (e.g., Braham et al. 1981) may play a role, numerous studies are in general agreement that the urban heat island (UHI) is responsible in some way (e.g., Bornstein and Lin 2000; Dixon and Mote 2003; Rozoff et al. 2003). These studies have found evidence that UHIs produce convergence zones that can initiate new convection.

Most previous work has focused on all forms of convective activity, with some studies including cells that reach a maximum reflectivity as low as 40 dBZ (e.g., Haberlie et al. 2015). Several recent studies have focused specifically on the impact urban areas may have on strong, deep convection capable of producing severe weather. Naylor and Sexton (2018) found that storm-based NWS warnings and the frequency of convective cells with a reflectivity of 50 dBZ or more are maximized on the downwind side of several large cities. Reames and Stensrud (2018) performed WRF simulations of a supercell and found that the strength of low-level rotation, as well as the track of the near-surface mesocyclone, can be impacted by the presence of a large city.

Results from METROMEX suggest that urban areas are more likely to enhance existing precipitation systems than to initiate new convective cells (e.g., Huff and Changnon 1973). A similar conclusion was reached by Shem and Shepherd (2009) in their analysis of two separate convective events over Atlanta, Georgia. Niyogi et al. (2011) also found observational evidence of storms changing structure when interacting with a city. Using a large radar-based climatology

of convective events over a 10-year period, they found that thunderstorms approaching Indianapolis, Indiana were more likely to change structure when passing over the city compared to thunderstorms passing over nearby rural regions. However, other studies have found strong evidence of urban-induced convective initiation (e.g., Bornstein and Lin 2000, Craig and Bornstein 2002; Dixon and Mote 2003; Haberlie et al. 2015). These initiation events are most often associated with warm humid air masses and synoptically benign conditions during the peak in summer. As pointed out by Haberlie et al. (2015), studies investigating the climatology of urban-induced convection are much less common in the literature than more general climatological studies of thunderstorm occurrence around large cities.

The goal of this study is to further investigate the impact of large urban areas on convective initiation and the occurrence of isolated deep convective storms capable of producing hazards such as flash floods, damaging winds, and hail. The primary focus area is Louisville, Kentucky. Previous research has shown that Louisville has one of the strongest UHIs in the U.S. (Debbage and Shepherd 2015). Since processes associated with UHIs are believed to be related to precipitation modification, it is possible that Louisville may have a detectable influence on area precipitation. An example of a summertime convective initiation event over Louisville, Kentucky on 10 July 2019 is shown in Figure 1. This cell developed during the afternoon on the eastern side of the city with no other convective activity in the vicinity. This cell remained relatively stationary as it grew in size over a period of approximately 40–50 min and reached a maximum radar reflectivity value ≥ 50 dBZ. After the storm propagated out of the city, it dissipated (not shown). The main goal of this study is to determine if events such as this are more common over Louisville than nearby rural areas.

This study differs from previous studies of urban-induced and urban-enhanced convection in several ways. First, we focus only on "strong" convective cells, with convective strength based on observed radar reflectivity. Second, many previous studies have focused only on warm season convection, while others have gone a step further to restrict their search to warm season events that occur under a specific type of airmass (e.g., Dixon and Mote 2003; Mote et al. 2007; Bentley et al. 2012; Haberlie et al. 2015). This study has no such restrictions. Any convective event that meets the specified criteria will be considered, regardless of the season in which it occurred, or the synoptic conditions associated with it. Finally, the focus of this current study is the initiation of new cells over the urban area itself. While many previous studies have found an increase in precipitation downwind of large cities, our goal is to examine the occurrence of strong, discrete convective activity over a large city.

2. Methodology

a. Identification of urban and rural cases

Data from the Severe Weather Data Inventory (SWDI; Ansari et al. 2009) are used to create a radar-based climatology of convective activity around a specified point from January 2003 through December 2019. The SWDI dataset includes the Level III "Storm Structure" product from National Weather Service WSR-88D radars, which contains information for identified cells such as time, latitude/longitude, maximum reflectivity, vertically integrated liquid water content, and cloud depth. These data have a temporal resolution of 5 minutes. For an analysis of Louisville and the surrounding area, data from the KLVX radar at Fort Knox, Kentucky are used.

To identify instances of strong, isolated convective activity over Louisville, we create a "cone of influence" relative to a particular location using a process described in Naylor and Sexton (2018). This creates fan-like areas emanating from the reference location in either direction (Figure

2). Similar approaches have been adopted by many previous studies involving urban precipitation anomalies (e.g., Huff and Changnon 1972; Shepherd and Burian 2003). The 'focus' area over Louisville (purple portion in Fig. 2) extends 25 km eastward from the point of origin and the 'control' area (blue portion of Fig. 2) extends 20 km westward from the point of origin. Since convection is discrete by its very nature, initiation of convection over a particular point on the surface does not necessarily mean that the properties of the underlying surface substantially impacted that development. To determine if isolated convective activity over Louisville is more common compared to nearby areas, the methodology described above was repeated at five rural points (herein RPs). At each of these selected RPs, focus and control areas were defined (centered on the latitude and longitude of the RP) and the SWDI dataset was searched for instances of strong convection in the focus area but not in the control area. Because cell detection and radar reflectivity are strongly influenced by distance from the radar, the RPs were chosen at points located at a similar distance from the KLVX radar as Louisville (Figure 2). The lowest possible radar beam height (assuming 0.5º elevation angle) within the various focus regions shown in Figure 2 ranges from approximately 300 m to 900 m.

The reference location and radial extent were chosen such that the majority of Louisville is contained within the focus area. The geometry of the focus region is intended to minimize non-urban land use within the shape. For example, if a semi-circle were chosen instead of a cone, the focus area would extend to areas 20 km directly north and south of the radial center. This would include a heavily forested area near Fort Knox, Kentucky and rural areas in southern Indiana. To be considered a strong isolated event, convection exceeding a predefined reflectivity threshold must be identified within the focus area with no detections of 30 dBZ or greater in the control area during a moving three-hour window. The radial extent of each cone was determined by trial and

141 error. The purpose of the control area is to identify and remove events with a) existing cells that
142 were advected over Louisville due to the prevailing winds and b) widespread convective initiation
143 over a large area.

144 Case selection was automated using a Python script to search the SWDI dataset for events
145 that met the defined criteria. Various reflectivity thresholds were tested and identified cases were
146 manually checked for consistency. It was found that lower reflectivity thresholds (such as 50 dBZ)
147 produced too many "false alarms"—cases where relatively weak cells met the maximum
148 reflectivity threshold for just a single scan. Choosing too large of a threshold limited the number
149 of available cases. Thus, 55 dBZ was chosen as an acceptable threshold to identify "strong"
150 convection. This threshold value yielded a reasonable number of events (116) while also limiting
151 the number of weaker convective events detected by the data-mining code.

152 Detected cases are a combination of discrete convective initiation as well as the
153 enhancement of existing, weak clouds. For example, it is possible for a weak, developing
154 convective cell with a reflectivity of less than 30 dBZ to move from the control region and then
155 intensify to greater than 55 dBZ in the focus region[1]. New cells may also be initiated directly in
156 the focus region without any prior weak cell detections in the control region. A manual inspection
157 of cases identified by the detection script revealed that the majority of cases involve the initiation
158 of a single cell near Louisville with no other convection within 30 km of the city—similar to the
159 event depicted in Figure 1. There are also several cases where an existing convective system
160 approaches Louisville without passing into the control area, and new cells initiate within the
161 defined focus region. It is also possible that a strong existing cell that developed well outside of

[1] Mecikalski and Bedka (2006) define convective initiation as having occurred when reflectivity of 35 dBZ or greater is detected by a WSR-88D radar. By that criteria, weak cells moving from the control area into the focus area before intensifying to 35 dBZ or more would be categorized as having initiated in the focus area.

Louisville could pass through one of the "gaps" between the focus and control regions, travel into the focus region and be labeled as an initiation event by the analysis code. A manual investigation revealed that this scenario was relatively rare and accounts for less than 10% of the total number of detections.

Statistical analysis was performed to determine if significant differences in convective activity exist between Louisville and the RPs. Statistical significance was investigated using permutation testing of yearly convective counts at each location (e.g., Wilks 2006). The test statistic used for the resampling method was the ratio of yearly mean isolated convective cases between the urban location and RPs (herein, $\overline{urb}/\overline{rur}$). For each RP, 100,000 randomly generated samples of the observed yearly convective urban and rural counts were created. For each sample, $\overline{urb}/\overline{rur}$ was calculated and the distribution of $\overline{urb}/\overline{rur}$ was compared to the observed value. The *p*-value was determined by the fraction of simulated $\overline{urb}/\overline{rur}$ values that exceeded the observed value. For comparison to the permutation method, the *p*-value was also calculated using the commonly used Wilcoxon signed-rank test for each location (Wilcoxon 1945).

b. Synoptic environments of cases

To investigate how cases are related to synoptic environments, a competitive neural network known as the Self Organizing Map (SOM, Kohonen 1989) was used to objectively classify 500 hPa geopotential height patterns from the North American Regional Reanalysis (NARR, Mesinger et al. 2006). For the sake of brevity, the reader is referred to Kennedy et al. (2016), Kennedy et al. (2019) and Wang et al. (2019) for details on the merits of SOMs. The training process for this study is most similar to Wang et al. (2019). Differences with this study include geographical area, the selection of training samples, and the use of only 500 hPa heights

184 (vs. combinations of atmospheric variables). In the latter case, additional variables did not improve
185 discrimination of urban vs. rural cases.

186 SOMs were created for the summer (June-July-August) from 00 UTC NARR height
187 patterns from 2003-2019. This subset of time (vs. the entire season) allowed us to emphasize
188 variability between quiescent and synoptically-active periods and also highlights a period when
189 the greatest difference in cases was observed (see Section 3a). Inclusion of patterns from other
190 months skewed results to more active patterns and led to larger classification errors. In total, 17
191 years of summer seasons provided 1564 training samples. Like these prior studies, NARR was
192 averaged to 1°×1° grid for a 15° latitude × 19° longitude region, but centered on Louisville, KY.
193 The height field was calculated as an anomaly from the domain average to prevent biases due to
194 seasonally dependent thermal thickness (Kennedy et al. 2016). Various size SOMs were created,
195 but the best balance between number of convective cases and variability expressed by the SOM
196 occurred for a 28-class, 7×4 map. Urban and rural cases were then classified to the SOM using the
197 minimum Euclidean distance for the NARR 3-hr time step closest in time.

198 **3. Results**

199 *a. Convective initiation near Louisville, Kentucky*

200 Using the criteria outlined above, 116 cases were identified over Louisville, Kentucky
201 during the period from 2003–2019 (Table 1). The total number of events at the RPs ranges from
202 62 (RP1) to 87 (RP4). The average (6.8) and median (7.0) values are also greater than at any of
203 the RPs. At RP1, the median is less than half of the Louisville value. To determine the statistical
204 significance of these results, permutation testing was completed using 100,000 randomly generated
205 samples. Figure 3 shows the distribution of the test statistic, $\overline{urb}/\overline{rur}$, at RPs 1–5[2]. At each

[2] For clarity and to prevent overlap, only rural locations 1–5 in Table 1 are shown.

location, the observed value of $\overline{urb}/\overline{rur}$ is located at the tail end of the randomly generated values. The one-sided *p*-values indicate that the observed differences are statistically significant at the 95% confidence level (or greater) for each of the five RPs (Table 1).

Convective events were grouped by month and the difference in monthly count between Louisville and each RP is was calculated (Figure 4). As expected, the largest differences in urban and rural counts occur during meteorological summer, with May through August typically being the months of peak difference. Although convective activity is less common at all locations during the cool season, Louisville appears to have less convective activity than several of the RPs during the winter and early spring. A comparison between the timing of convective events over Louisville and the RPs is shown in Figure 5. Differences are largest between 1800 and 0200 UTC, indicating that Louisville experiences more convective activity (compared to the surrounding RPs) beginning in the afternoon and ending before midnight local time. This time frame is similar to that identified by Haberlie et al. (2015) for convective initiation around Atlanta, GA but slightly longer than the time period of maximum urban-associated rainfall over Atlanta identified by McLeod et al. (2017). At four of the five RPs shown in Figure 5, the difference is largest between 1800-2400 UTC. However, Figure 5 also shows that each RP experiences more convective activity overnight and during the morning hours relative to Louisville. This difference peaks sometime between 0400-1000 UTC.

Figure 6 shows time series of urban/rural convective activity during each year of the study period. The most convective events over Louisville occurred in 2006, 2010. Overall, there is no detectable upward or downward trend in the number of events per year. For the RPs, there is some shared signal, but not always. For example, all locations experienced a relatively high amount of convective activity in 2010 and a lower amount in 2013. Similar patterns were also evident for

Louisville during these years. At each RP, there is at least one year where convective activity was the same or greater than Louisville. RP4 has the greatest number of years when this occurs (7), while RP1 has the least (2).

b. Partitioning of events by 500hPa height patterns

The summer months of June–August were used to classify climatological 500 hPa height patterns surrounding Louisville, Kentucky from 2003–2019 (Figure 7). The SOM captures variability across this season with patterns ranging from a stronger flow on the left side of the feature map and quiescent conditions on the right (Figure 7a). In total, 131 urban and rural cases were classified from the summer months to nodes on the SOM (Figure 7b). Cases were least likely to occur on the upper-left side of the SOM; these patterns have strong NW flow aloft with the trough axis located to the east of Louisville, Kentucky. In these situations, subsidence is generally expected from quasi-geostrophic theory as there is anticyclonic vorticity advection increasing with height. Cases occurred across the remainder of the SOM with cases ranging from near-zonal flow (bottom center), to southwesterly flow (bottom right), to weak flow with various positions with respect to the thermal ridge (upper right). The speckled nature of case counts in the bottom of the SOM is more likely to be tied to sampling issues vs. true neighboring class variability. Rather, we focus our attention to broad changes across the SOM (e.g., strong vs. weak flow).

Urban and rural cases were separated to understand whether they have preferential 500 hPa patterns of occurrence (Figure 8). To limit issues with sampling, results are plotted as the fraction of total cases. While sampling cannot be completely negated (e.g., noise in fractions seen along the perimeter with urban cases), a clear shift in patterns can be seen. Overall, urban cases are more likely under quiescent conditions on the right-hand side of the SOM (Figure 8a.) while rural cases are more likely under synoptically active time periods (Figure 8b.).

c. Other cities

The results show that Louisville experiences significantly more days with isolated deep convective storms compared to nearby rural areas. However, a causal relationship for this has not been established. While it is likely that urban processes are responsible for this difference, it is also possible that other features—such as topographical variations—play a role. To further investigate this possibility, the procedure described in Section 3a was repeated for Nashville, Tennessee and Cincinnati, Ohio with some modifications to the geometry of the focus/control areas (Figure 9). For Nashville, the radial extent of the focus and control areas is 25 km, and 20 km, respectively. For Cincinnati, the limits were 35 km and 30 km. Data from the KILN radar were used for Cincinnati and surrounding RPs, while KOHX radar data were used for Nashville and surrounding RPs. The range of possible radar beam heights for Nashville and surrounding RPs is approximately 100 m to 500 m within the focus regions. For Cincinnati (and RPs), the lowest possible beam height ranges from 500 m to 2000 m. In addition to the five RPs identified around Cincinnati, a sixth location at 39.9697º latitude and -83.1691º longitude was included (Figure 9b). The focus area of this location extends over the Columbus, Ohio metropolitan area (herein this point is referred to as CBS). The purpose of this location is to directly compare convective activity over two different urban areas, both of which are approximately the same distance from the same radar.

The total number of isolated convective events over Nashville is 175 and values over the RPs range from 132 to 146 (Table 2). Figure 10 shows the results from the permutation resampling and the *p*-values from this analysis are shown in Table 2. At four of the five RPs, the difference in isolated convective activity (relative to Nashville) is statistically significant at the 95% confidence level when significance was determined by the permutation method. RP2 (*p*-value of 0.056) was

the only comparison point where differences were not significant at the 95% confidence interval. When the Wilcoxon signed-rank test was used, a statistically significant difference in convective activity (at the 95% confidence interval) was found at three of the RPs, with RP2 and RP4 being the locations that were not significantly different compared to Nashville. Differences in convective activity between the urban and rural environment tend to be maximized in June and July (Fig. 11), which is a narrower time frame than was found for Louisville, where peak differences relative to the various RPs occurred from May through August.

Cincinnati had 104 total events over the study period, which was the smallest of the three cities analyzed (Table 2). The total number of urban convective events over Cincinnati is greater than each of the five comparison RPs as well as the location over Columbus, Ohio (CBS). The results from the permutation resampling were statistically significant at the 95% confidence interval (Figure 12, Table 2) at four of the five RPs. As was the case with Nashville, the lone comparison RP that was not statistically significant (RP2; *p*-value of 0.054) was slightly outside the defined confidence interval. Interestingly, the CBS location yielded the most convective events of all of the comparison locations. Differences in convective activity between Cincinnati and CBS were not statistically significant, with *p*-values of 0.22 and 0.23 from the permutation testing and Wilcoxon methods. Figure 13 shows that differences in convective activity between Cincinnati and the RPs is maximized in July and August (Figure 13), which is slightly later than the peak differences observed for Louisville and Nashville.

4. Discussion

The results show that Louisville experiences strong, isolated convective activity more often than surrounding rural locations. This activity is more likely under quiescent conditions when there

298 is weaker synoptic forcing. In order to determine if the results from Louisville were dominated by
299 the impact of urban processes or may have been influenced by other local factors, the procedure
300 was repeated for two nearby large cities— Nashville, Tennessee and Cincinnati, Ohio.
301 Indianapolis, Indiana was also considered for analysis, however the KIND radar is located only
302 about 15 km from the downtown center of Indianapolis. This made it impossible to define RP
303 focus regions that were approximately the same distance from the radar as the urban focus region
304 and did not overlap with the urban focus region. This presents a limitation of our methodology—
305 it cannot be used in cities where the nearest WSR-88D is very close to the city itself.
306 The results from the analysis of Nashville and Cincinnati also revealed greater convective
307 activity in these cities compared to nearby rural areas, although each city had one RP where
308 convective activity was not statistically different from that in the comparison urban area at the
309 95% confidence interval. Also, Cincinnati presented a unique opportunity since the KILN radar is
310 nearly halfway between Cincinnati and Columbus, Ohio. A sixth comparison site placed such that
311 the focus area extended over the Columbus region. This location produced the smallest difference
312 in convective activity (relative to Cincinnati) and the largest *p*-value of all tested points. This
313 finding provides further evidence that convective initiation is enhanced over urban areas.
314 To examine the sensitivity of the results to the geometry of the control and focus areas, two
315 additional experiments were completed for Louisville (not shown). In one test, the control and
316 focus areas were rotated to be oriented from southwest to northeast—in better agreement with the
317 mean summer wind direction and storm motion[3]. This slightly changed the total number of events
318 at each location but the urban-rural difference in convective activity remained statistically

[3] Wind climatology was determined using data from the Iowa Environmental Mesonet website: https://mesonet.agron.iastate.edu/sites/windrose.phtml?station=LOU&network=KY_ASOS

significant at each RP. In the second test, we removed the 'gaps' between the control and focus area by increasing the size of the control area. This resulted in substantially fewer events at each location do the more stringent criteria. For example, 71 isolated events were identified over Louisville using this method whereas our original method yielded 116 events (see Table 2). With this method, statistically significant differences in convective activity were found at four of the five RPs. Only RP1 did not produce a statistically significant result.

Since differences in urban-rural convective activity were strongest during the summer, the analysis was repeated considering only convective activity during the 'warm' season, which we defined as May–September (not shown). This did not alter the significance of the results. For Louisville and Cincinnati, the number of RPs with significantly less convective activity remained the same. For Nashville, only three of the RPs yielded a statistically significant result when considering only the warm season, compared with four out of five when considering the full dataset.

While the findings of this study indicate that Louisville and the other cities tested experience more convective activity compared to nearby rural locations, none of the findings establish a physical mechanism for the increased convection or provide any assistance in predicting future convective events within the city. The University of Louisville is currently in the process of deploying a network of surface-based weather stations around Louisville to study its UHI and other urban effects. The network is composed of Davis Vantage Pro2 stations located throughout the city. Observations from the partially completed network were examined to determine if a physical mechanism for convective initiation could be found and if urban-induced convective activity may be forecasted ahead of time. Figure 14 shows a surface analysis of eight stations within the network, as well as observations from the ASOS station at Bowman Field, from the afternoon of

10 July 2019. Note that this is the same date as the convective initiation event shown in Figure 1. Figure 14a shows the surface conditions at 18 UTC. The highest temperatures are located within the northeast corner of the city and with lower values found in the south and southeast portions of Louisville. Winds are less than 5 knots, with one of the stations in the eastern half of the city indicating westerly/southwesterly flow. By 19 UTC (Figure 14b), westerly winds increase in strength at locations in the northwest portion of the city. Farther to the east, the Bowman Field ASOS station reports winds from the southeast at 10 knots. To the south of Bowman Field, winds are from the southwest. The shifting winds indicate a localized region of convergence near the center of Louisville. By 1917 UTC reflectivity values of 30-40 dBZ begin to appear within this prospective region of convergence, and by 1917 UTC, reflectivity values of over 50 dBZ are present (Figure 1). This agrees with Bornstein of Lin (2000), who found evidence of near-surface convergence preceding urban initiated convection in Atlanta, Georgia. While these initial results are promising, research involving the use of this observation network to anticipate convective development in real-time is ongoing.

5. Summary and Conclusions

This study investigated differences in the occurrence of strong, isolated convective cells between Louisville and five select nearby rural locations. Compared to five rural locations used for comparison, Louisville experienced significantly more strong isolated convective events over the period 2003-2019. Differences in convective activity between Louisville and the surrounding rural areas are largest during meteorological summer, with a peak difference from May through August at most locations. Furthermore, it was found that relative to the rural locations, Louisville experiences more convective activity beginning in the afternoon and ending before midnight.

Activity over the city is more likely during synoptically quiescent conditions. These findings agree with those of Haberlie et al. (2015) and their analysis of urban-induced convective initiation events in Atlanta, Georgia. In contrast, the rural locations tend to experience more convection during the morning hours and upper-level patterns suggested events were more likely tied to synoptic-scale forcing.

A similar analysis was completed for Nashville, Tennessee and Cincinnati, Ohio. Each of these cities experienced more frequent convective activity over the study period than their five nearby rural locations. However, for both these cities differences in convective activity are statistically significant at four of the five rural locations. It was also found that the peak differences in convective activity, relative to the surrounding rural regions, occur in July–August for Cincinnati and June–July for Nashville.

Further research is needed to explore the physical mechanism(s) responsible for these observed differences. Based on the time of day and time of year that the differences are maximized, it is likely that the urban heat island plays a substantial role. However, it is possible that non-urban effects such as topography are impacting convective activity around these cities. Future work will focus on analyzing observations from the surface-based network discussed in Section 4 in combination with convective-allowing WRF simulations to explore these remaining questions.

6. Acknowledgements

A portion of this research was sponsored by the National Science Foundation, grant number AGS-1953791. Kennedy was supported by the National Science Foundation under NSF EPSCoR Track-1 Cooperative Agreement OIA 1355466. We thank the anonymous reviewers whose helpful comments and suggestions greatly improved an earlier version of this work.

388 **References**

389 Ansari, S., M. Phillips, and S. Del Greco, 2009: NEXRAD Severe weather signatures in the NOAA
390 Severe Weather Data Inventory, *34th Conference on Radar Meteorology*, Williamsburg, VA.

391 Bentley, M. L., J. A. Stallins, and W. S. Ashley, 2012: Synoptic environments favourable for urban
392 convection in Atlanta, Georgia. *Int. J. Climatol.*, **32**, 1287–1294, doi:10.1002/joc.2344.

393 Bornstein, R., and Q. Lin, 2000: Urban heat islands and summertime convective thunderstorms in
394 Atlanta: Three case studies. *Atmos. Environ.*, **34**, 507–516, doi:10.1016/S1352-
395 2310(99)00374-X.

396 Braham, R. R., R. G. Semonin, A. H. Auer, and S. A. Changnon, 1981: Summary of urban effects
397 on cloud and rain. *METROMEX: A Review and Summary*, *Meteor. Monogr*., No 40, Amer.
398 Meteor. Soc., 141–152.

399 Changnon, S. A, F. A. Huff, and R. G. Semonin, 1971: METROMEX: an investigation of
400 inadvertent weather modification. *Bull. Am. Meteorol. Soc.*, **52**, 958–968, doi:10.1175/1520-
401 0477(1971)052<0958:MAIOIW>2.0.CO;2.

402 Changnon, S. A., F. A. Huff, P. T. Schickedanz, and J. L. Vogel, 1977: Summary of METROMEX,
403 Volume 1: Weather Anomalies and Impacts. Illinois State Water Survey, Urbana, Bulletin
404 62.

405 Craig, K. J., and R. D. Bornstein, 2002: MM5 simulations of urban induced convective
406 precipitation over Atlanta. *4th AMS Symposium on the Urban Environment*, Norfolk, VA, 5–
407 6.

408 Debbage, N., and J. M. Shepherd, 2015: The urban heat island effect and city contiguity. *Comput.*
409 *Environ. Urban Syst.*, **54**, 181–194, doi:10.1016/j.compenvurbsys.2015.08.002.

410 Dixon, P. G., and T. L. Mote, 2003: Patterns and causes of Atlanta's urban heat island–initiated
411 precipitation. *J. Appl. Meteorol.*, **42**, 1273–1284, doi:10.1175/1520-
412 0450(2003)042<1273:PACOAU>2.0.CO;2.

413 Ganeshan, M., R. Murtugudde, and M. L. Imhoff, 2013: A multi-city analysis of the UHI-influence
414 on warm season rainfall. *Urban Clim.*, **6**, 1–23, doi:10.1016/j.uclim.2013.09.004.

415 Haberlie, A. M., W. S. Ashley, and T. J. Pingel, 2015: The effect of urbanisation on the climatology
416 of thunderstorm initiation. *Q. J. R. Meteorol. Soc.*, **141**, 663–675, doi:10.1002/qj.2499.

417 Hjelmfelt, M. R., 1982: Numerical simulation of the effects of St. Louis on mesoscale boundary-
418 layer airflow and vertical air motion: Simulations of urban vs non-urban effects. *J. Appl.*
419 *Meteorol.*, **21**, 1239–1257, doi:10.1175/1520-0450(1982)021<1239:NSOTEO>2.0.CO;2.

Huff, F. A., and S. A. Changnon, 1973: Precipitation modification by major urban areas. *Bull. Am. Meteorol. Soc.*, **54**, 1220–1232, doi:10.1175/1520-0477(1973)054<1220:PMBMUA>2.0.CO;2.

Jin, M., J. M. Shepherd, and M. D. King, 2005: Urban aerosols and their variations with clouds and rainfall: A case study for New York and Houston. *J. Geophys. Res. D Atmos.*, **110**, 1–12, doi:10.1029/2004JD005081.

Kennedy, A.D., X.Dong, and B.Xi, 2016: Cloud fraction at the ARM SGP site: Reducing uncertainty with self-organizing maps. *Theor. Appl. Climatol.*, **124**, 43-54.

Kennedy, A. D., A. Trellinger, T. Grafenauer, and G.Gust, 2019: A climatology of atmospheric patterns associated with Red River valley blizzards. *Climate*, 7, **66**, https://doi.org/10.3390/cli7050066.

Kohonen, T., 1989: *Self-Organization and Associative Memory*. 3rd ed. Springer-Verlag, 312 pp.

Liu, J., Niyogi, D., 2019: Meta-analysis of urbanization impact on rainfall modification. *Sci Rep* **9,** 7301, https://doi.org/10.1038/s41598-019-42494-2

McLeod, J., M. Shepherd, and C. E. Konrad, 2017: Spatio-temporal rainfall patterns around Atlanta, Georgia and possible relationships to urban land cover. *Urban Clim.*, **21**, 27–42, https://doi.org/https://doi.org/10.1016/j.uclim.2017.03.004.

Mecikalski, J. R. and K. M. Bedka, 2006: Forecasting convective initiation by monitoring the evolution of moving cumulus in daytime GOES imagery. *Mon. Wea. Rev.*, **134**, 49–78. https://doi.org/10.1175/MWR3062.1

Mote, T. L., M. C. Lacke, and J. M. Shepherd, 2007: Radar signatures of the urban effect on precipitation distribution: A case study for Atlanta, Georgia. *Geophys. Res. Lett.*, **34**, 2–5, doi:10.1029/2007GL031903.

Naylor, J., and A. Sexton, 2018: The Relationship between severe weather warnings, storm reports, and storm cell frequency in and around several large metropolitan areas. *Weather Forecast.*, **33**, 1339–1358, doi:10.1175/waf-d-18-0019.1.

Niyogi, D., P. Pyle, M. Lei, S. P. Arya, C. M. Kishtawal, M. Shepherd, F. Chen, and B. Wolfe, 2011: Urban modification of thunderstorms: An observational storm climatology and model case study for the Indianapolis urban region. *J. Appl. Meteorol. Climatol.*, **50**, 1129–1144, doi:10.1175/2010JAMC1836.1.

Ochoa, C. A., A. I. Quintanar, G. B. Raga, and D. Baumgardner, 2015: Changes in intense precipitation events in Mexico City. *J. Hydrometeorol.*, **16**, 1804–1820, doi:10.1175/JHM-D-14-0081.1.

453 Reames, L. J., and D. J. Stensrud, 2018: Influence of a Great Plains urban environment on a
454 simulated supercell. *Mon. Weather Rev.*, 1437–1462, doi:MWR-D-17-0284.1.

455 Rozoff, C. M., W. R. Cotton, and J. O. Adegoke, 2003: Simulation of St. Louis, Missouri, land
456 use impacts on thunderstorms. *J. Appl. Meteorol. Climatol.*, **42**, 716–738, doi:10.1175/1520-
457 0450(2003)042<0716:SOSLML>2.0.CO;2.

458 Shem, W., and M. Shepherd, 2009: On the impact of urbanization on summertime thunderstorms
459 in Atlanta: Two numerical model case studies. *Atmos. Res.*, **92**, 172–189,
460 doi:10.1016/j.atmosres.2008.09.013.

461 Shepherd, J. M., and H. Pierce, 2002: Rainfall modification by major urban areas: Observations
462 from spaceborne rain radar on the TRMM satellite. *J. Appl. Meteorol.*, **41**, 689–701, doi:Doi
463 10.1175/1520-0450(2002)041<0689:Rmbmua>2.0.Co;2.

464 Shepherd, J. M., and S. J. Burian, 2003: Detection of urban-induced rainfall anomalies in a major
465 coastal city. *Earth Interactions*, **7,** 1–14.

466 Stallins, J. A., J. Carpenter, M. L. Bentley, W. S. Ashley, and J. A. Mulholland, 2013: Weekend–
467 weekday aerosols and geographic variability in cloud-to-ground lightning for the urban region
468 of Atlanta, Georgia, USA. *Reg. Environ. Chang.*, **13**, 137–151, doi:10.1007/s10113-012-
469 0327-0.

470 Thielen, J., W. Wobrock, A. Gadian, P. G. Mestayer, and J. D. Creutin, 2000: The possible
471 influence of urban surfaces on rainfall development: A sensitivity study in 2D in the meso-γ-
472 scale. *Atmos. Res.*, **54**, 15–39, doi:10.1016/S0169-8095(00)00041-7.

473 van den Heever, S. C., and W. R. Cotton, 2007: Urban aerosol impacts on downwind convective
474 storms. *J. Appl. Meteorol. Climatol.*, **46**, 828–850, doi:10.1175/JAM2492.1.

475 Wang, J., X. Dong, A. Kennedy, B. Hagenhoff, and B. Xi, 2019: A regime-based evaluation of
476 Southern and Northern Great Plains warm-season precipitation events in WRF. *Wea.*
477 *Forecasting*, **34**, 805–831, https://doi.org/10.1175/WAF-D-19-0025.1.

478 Wilcoxon, F., 1945: Individual comparisons by ranking methods, *Biometrics Bulletin*, **1**, 80-
479 83. doi:10.2307/3001968

480 Wilks, D. S., 2006: *Statistical Methods in the Atmospheric Sciences*. 2nd ed. Elsevier, 627 pp.

481

482

483

484

Tables

Table 1. Summary of convective activity at Louisville, Kentucky and each of the nearby rural locations (RPs). The latitude and longitude values represent the origin point of the focus and control regions. The *p*-value column represents the one-sided value calculated from permutation testing of $\overline{urb}/\overline{rur}$. The Wilcoxon *p*-value column represents the *p*-value from a Wilxocon signed-rank test. Statistically significant differences (as determined by *p*-value) at the 95% confidence level or greater are italicized and bold.

Location	Latitude	Longitude	Total Events	Average	Median	p-value	Wilcoxon p-value
Louisville	38.2211	-85.8211	116	6.8	7		
RP1	38.2195	-86.5935	62	3.6	3	***0.00005***	***0.006***
RP2	37.8332	-86.6332	77	4.5	5	***0.006***	***0.006***
RP3	37.5589	-86.2859	78	4.6	5	***0.004***	***0.002***
RP4	37.5185	-85.7295	87	5.1	5	***0.03***	***0.02***
RP5	37.7071	-85.4441	74	4.3	5	***0.003***	***0.007***

Table 2. Same as Table 1, except for Cincinnati, Ohio and Nashville, Tennessee.

Location	Latitude	Longitude	Total Events	Average	Median	p-value	Wilcoxon p-value
Nashville	36.214	-86.8215	175	10	10		
RP1	36.4779	-86.5905	143	8.4	8	***0.045***	***0.04***
RP2	36.3945	-86.84	146	8.6	9	0.056	0.054
RP3	36.0201	-86.6546	136	8	8	***0.017***	***0.03***
RP4	36.0956	-86.3415	145	8.5	8	***0.047***	0.08
RP5	36.3945	-86.3394	132	7.7	7	***0.012***	***0.02***
Location	**Latitude**	**Longitude**	**Total Events**	**Average**	**Median**	**p-value**	**Wilcoxon p-value**
Cincinnati	39.2031	-84.712	104	6.1	6		
RP1	38.6428	-84.3979	70	4.1	4	***0.008***	***0.012***
RP2	39.5923	-84.9523	58	3.4	3	***0.001***	***0.007***
RP3	40.0927	-84.5832	76	4.5	4	***0.03***	***0.04***
RP4	39.3382	-82.8723	82	4.8	5	0.054	0.08
RP5	38.5272	-83.7555	70	4.1	4	***0.008***	***0.02***
CBS	39.9697	-83.1691	89	5.2	4	0.22	0.23

Figures

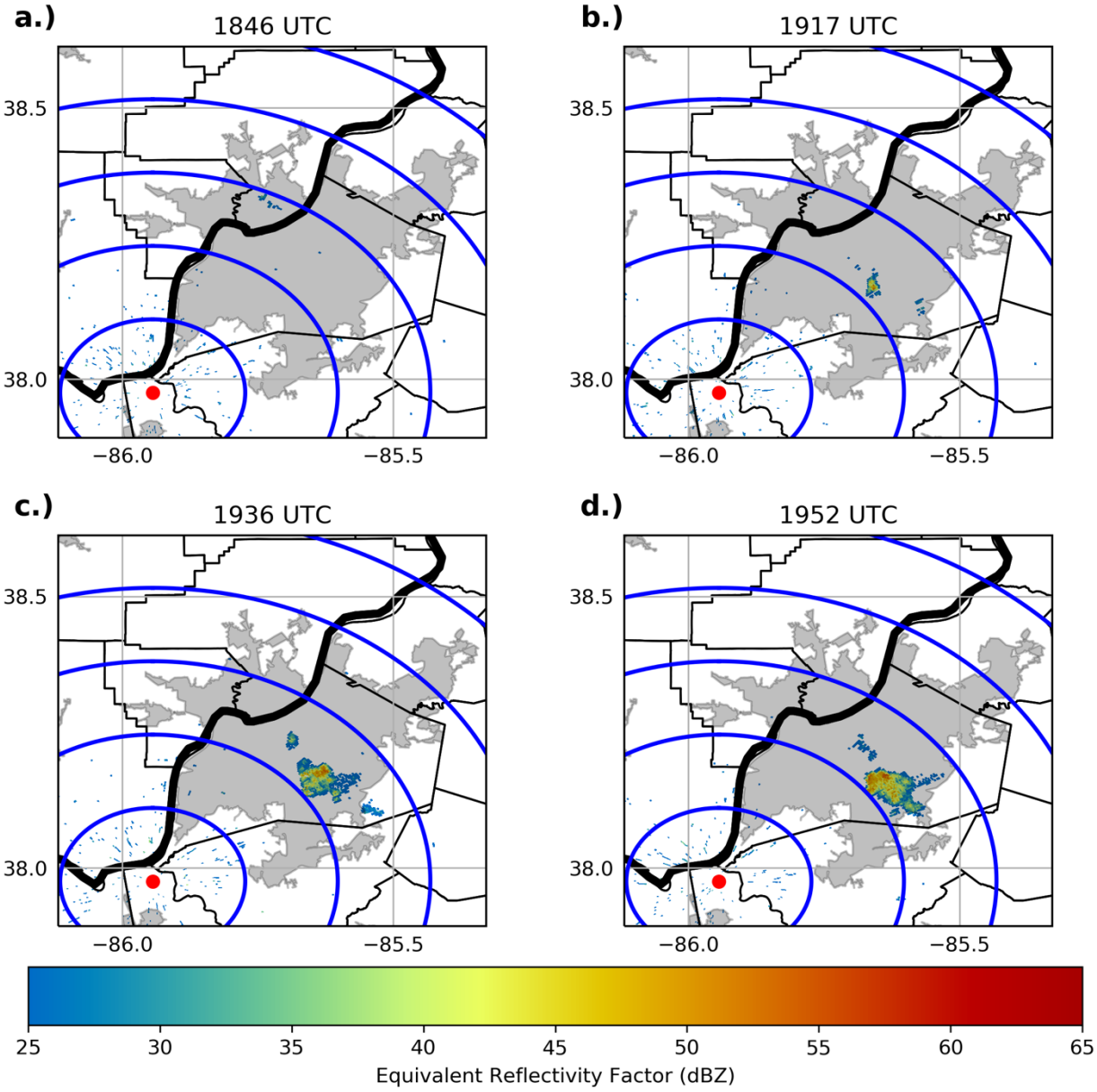

Figure 1. Radar observations of a convective initiation event over Louisville, KY from 10 July 2019. Displayed is base tilt (0.5°) equivalent reflectivity factor from the KLVX WSR-88D radar for a.) 1846, b.) 1917, c.) 1936, and d.) 1952 UTC. Blue lines are range rings drawn in intervals of 15 km while the red dot is the location of KLVX. Urban areas as identified by the U.S. Census Bureau are shaded in grey. The thick black line is the KY/IN border (Ohio River) and the thinner black lines represent county boundaries.

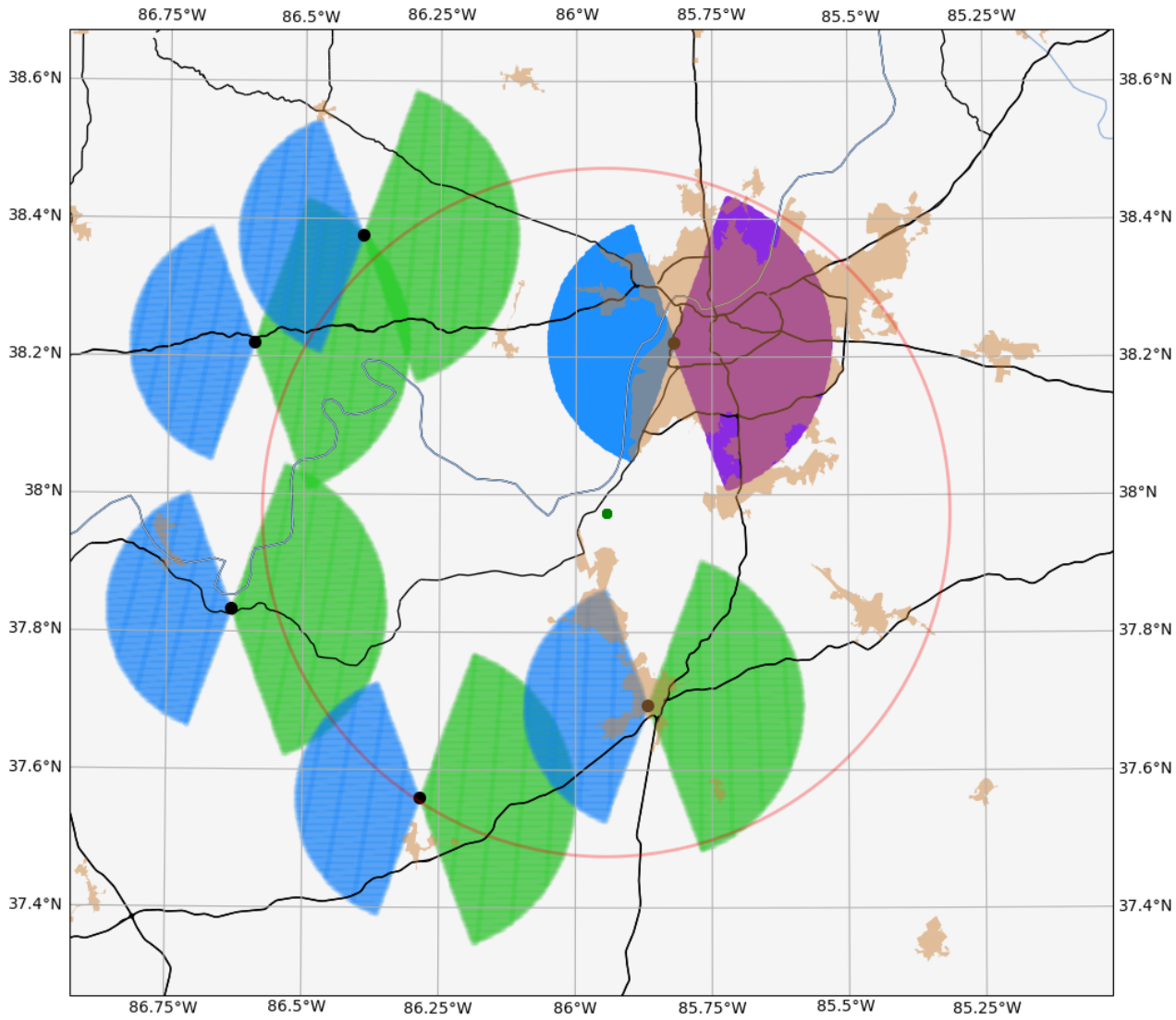

Figure 2. Map showing the relative positions of Louisville, Kentucky, the KLVX WSR-88D (green dot), and the five RPs used for comparison. The urban focus area over Louisville is indicated in purple, and the control area is in blue. For each RP, the focus area is in green and the control area in blue. The red ring represents a circle centered on the KLVX radar to indicate the relative radar distance of each of the focus areas. U.S. Census Bureau urban areas are shaded in orange. The black lines are major area roads, and the blue line is the Ohio River.

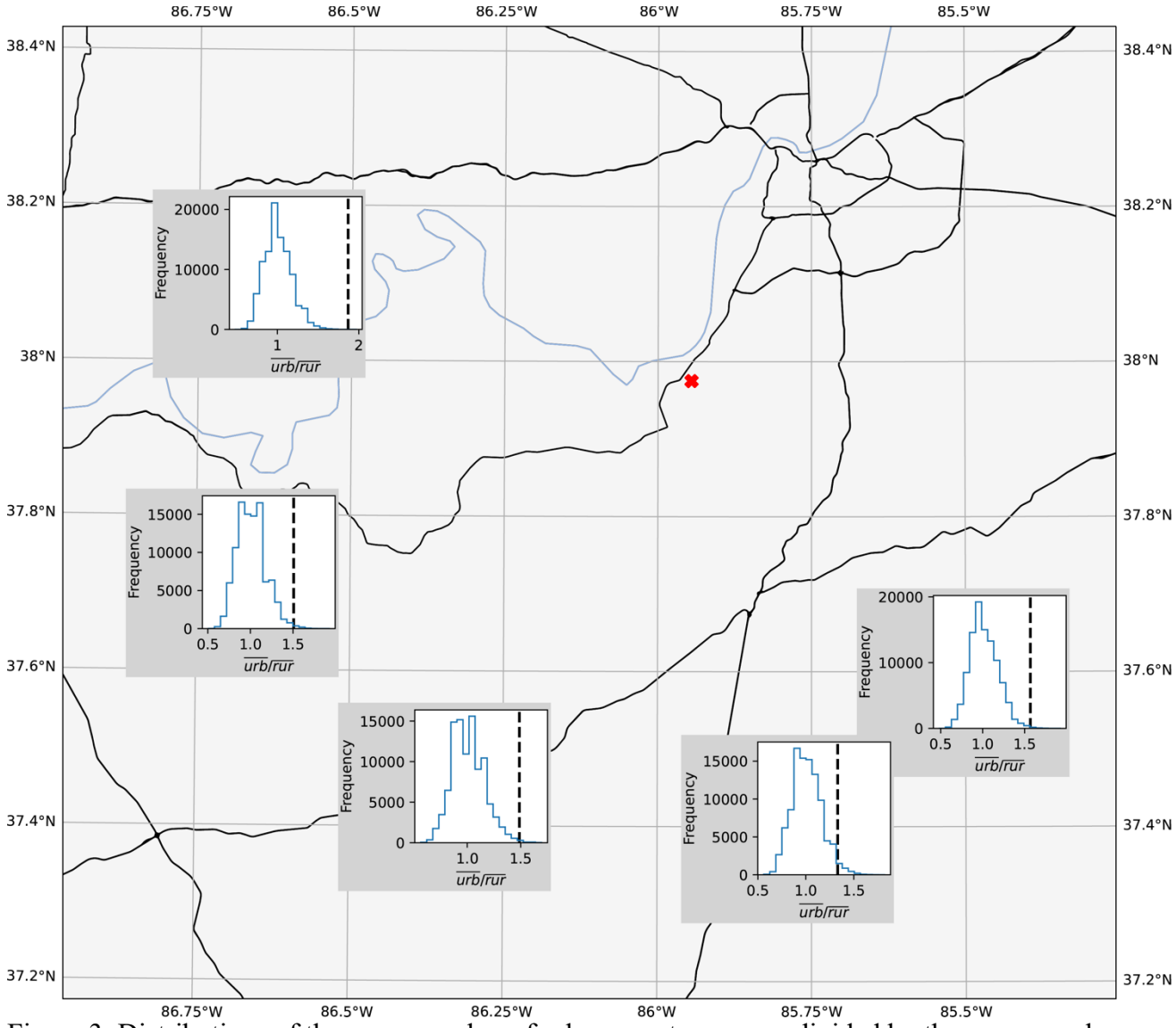

Figure 3. Distributions of the mean number of urban events per year divided by the mean number of rural events per year at each RP. Distributions are based on permutation testing of 100,000 samples. The vertical dotted black line indicates the observed ratio of the mean values at each RP. The red x represents the location of the KLVX radar. Black and blue lines are the same as in Figure 2.

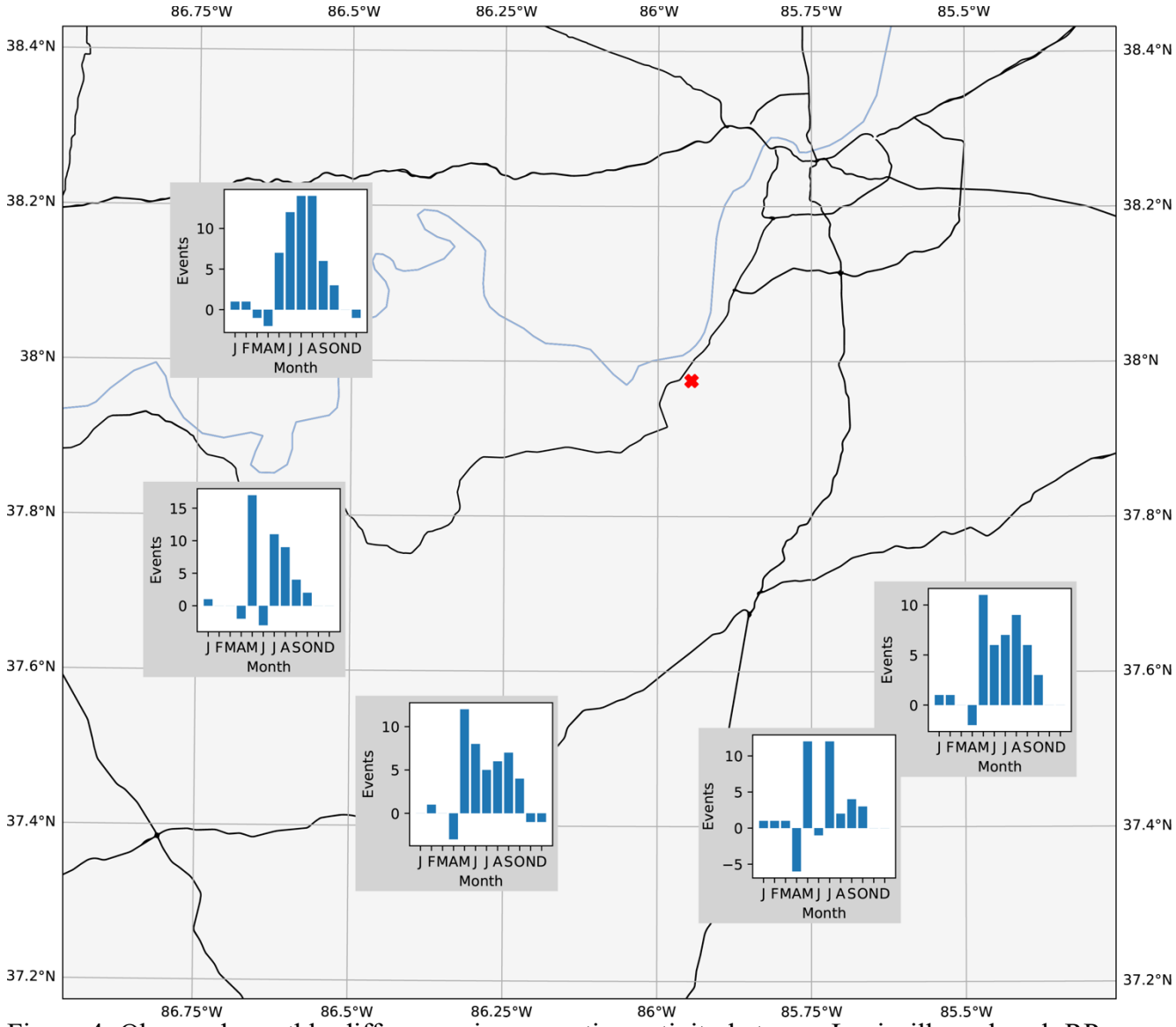

Figure 4. Observed monthly differences in convective activity between Louisville and each RP. Lines and markers are the same as in Figure 3.

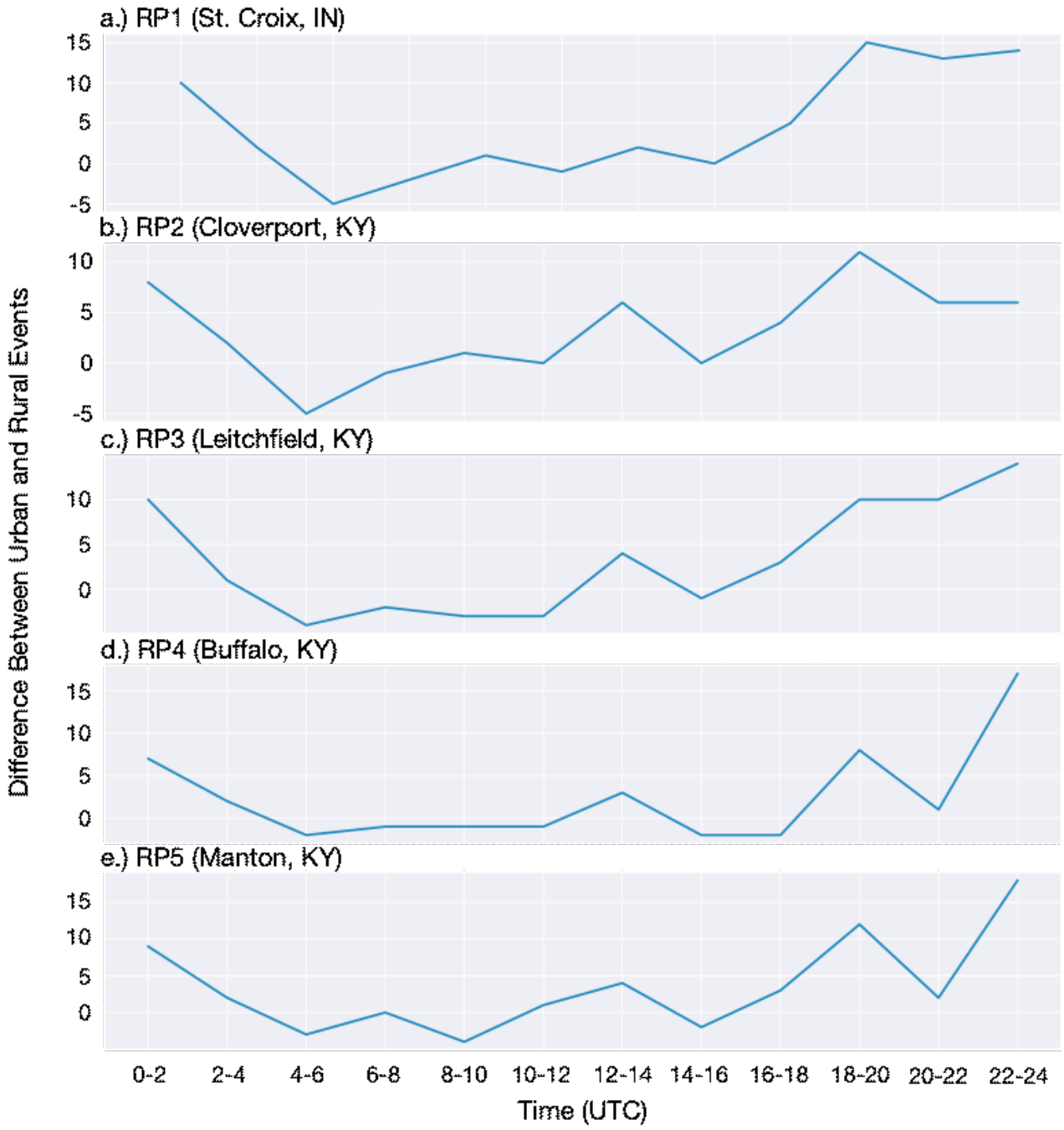

Figure 5. Differences in convective activity between Louisville and each RP as a function of time of day.

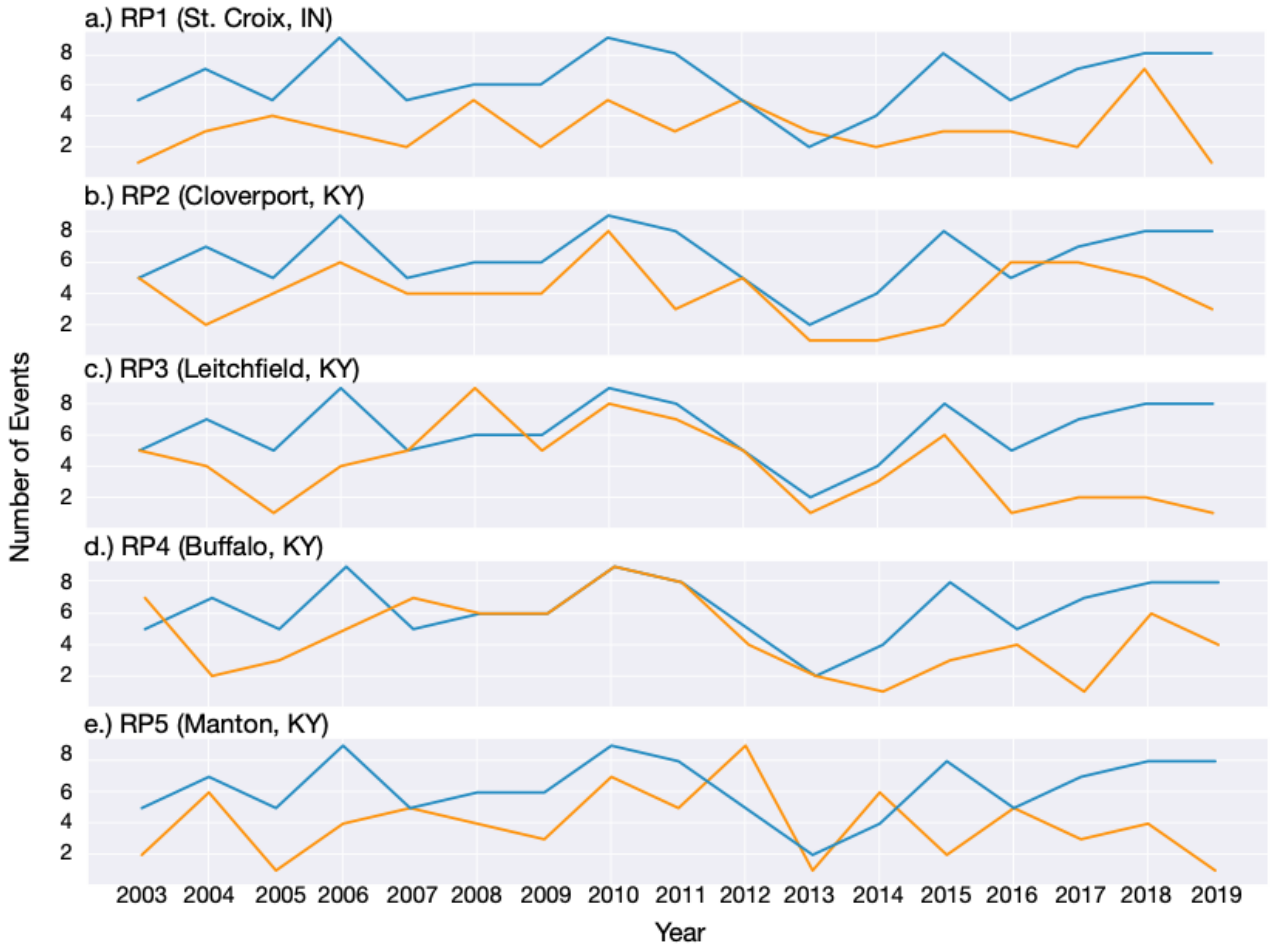

Figure 6. Time series of convective events per year at Louisville (blue line in each panel) and the designated RPs (orange line).

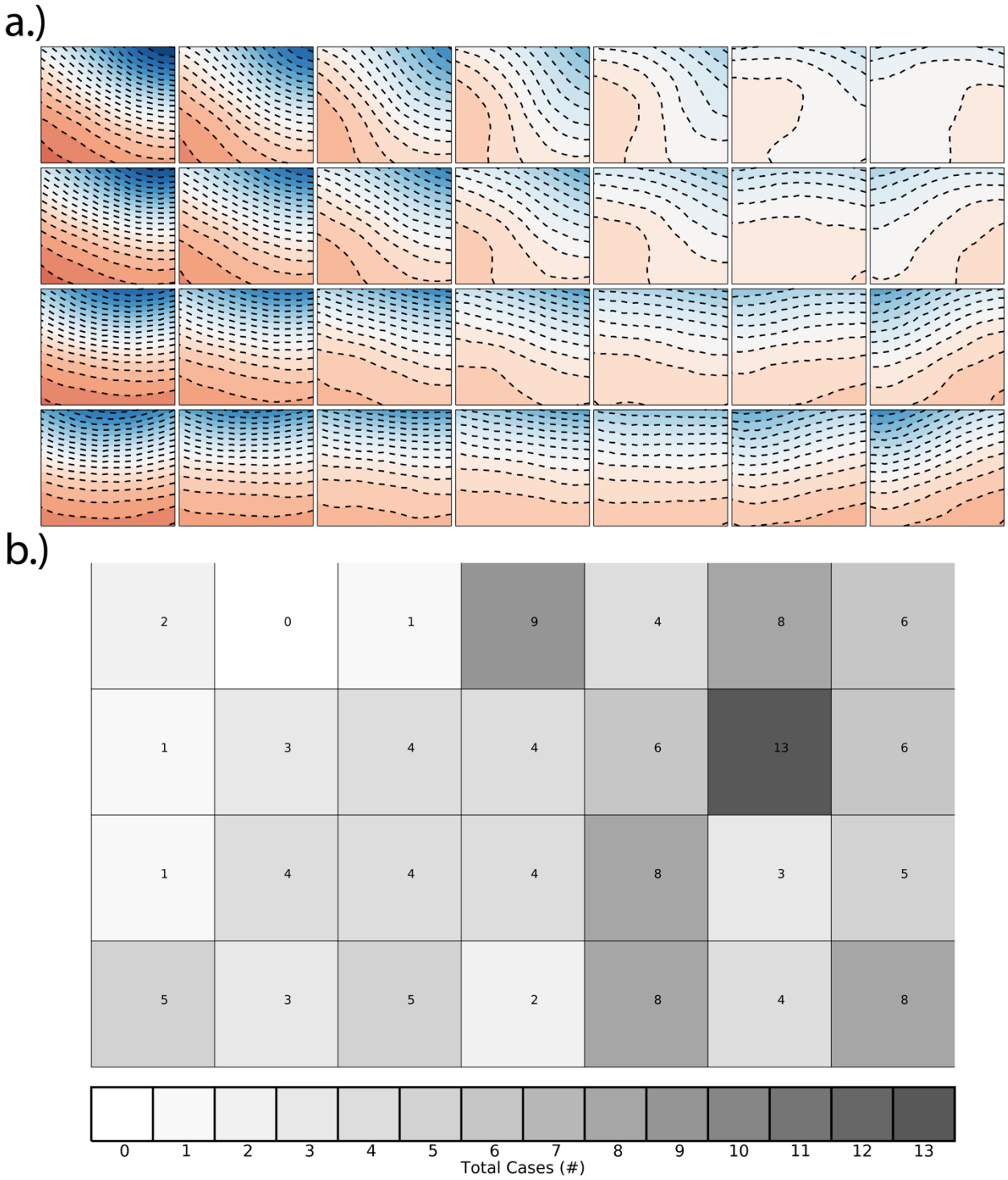

Figure 7. a.) 500 hPa height anomalies for the 7×4, 28-class SOM. Warmer (cooler) colors represent positive (negative) anomalies. a.) Total case count for the SOM. The total number of cases within the SOM is 131.

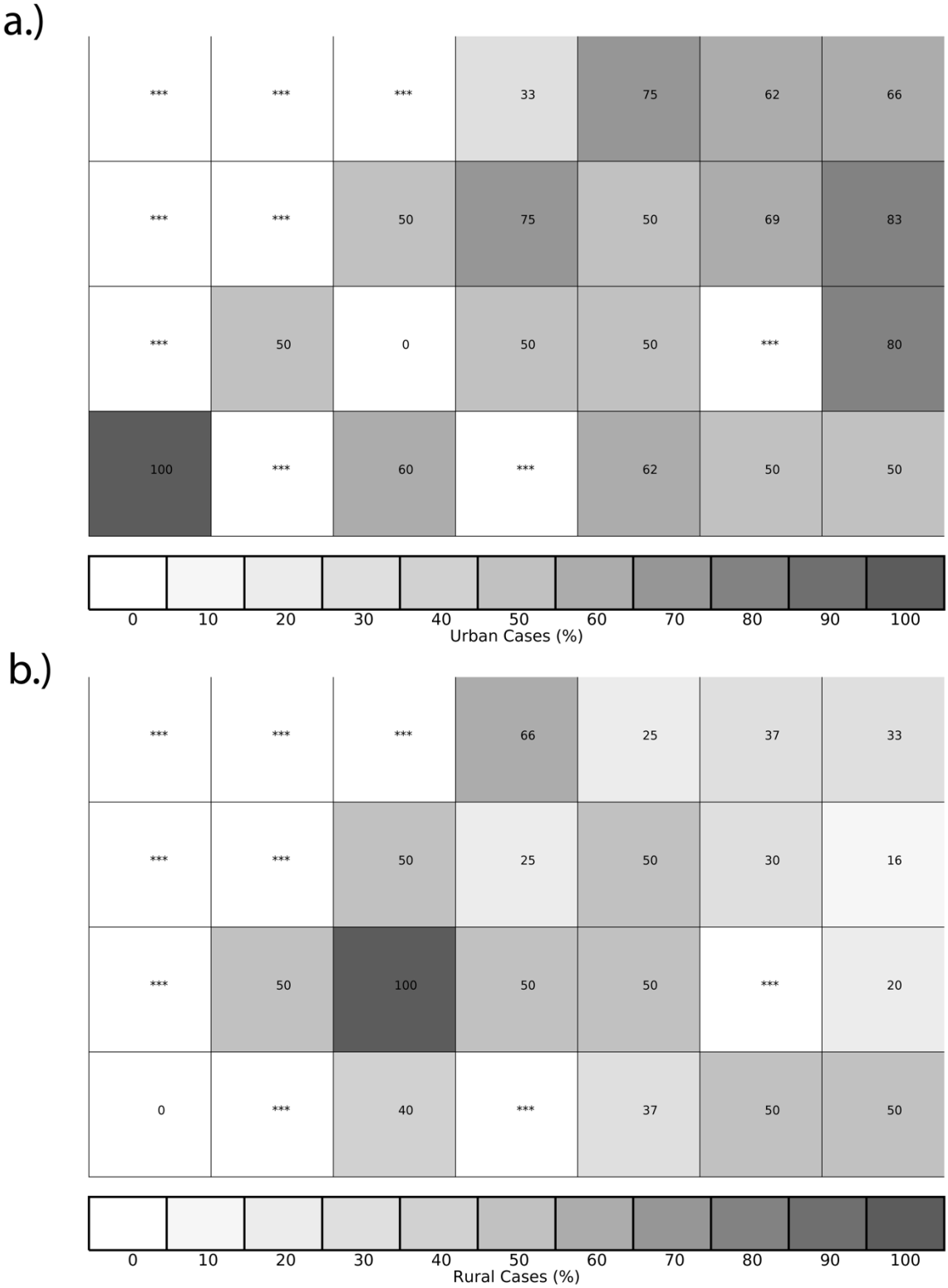

Figure 8. Fraction of a.) Urban and b.) Rural cases for the 28-class SOM shown in Figure 8. Nodes with three or less cases are masked and denoted with '***'.

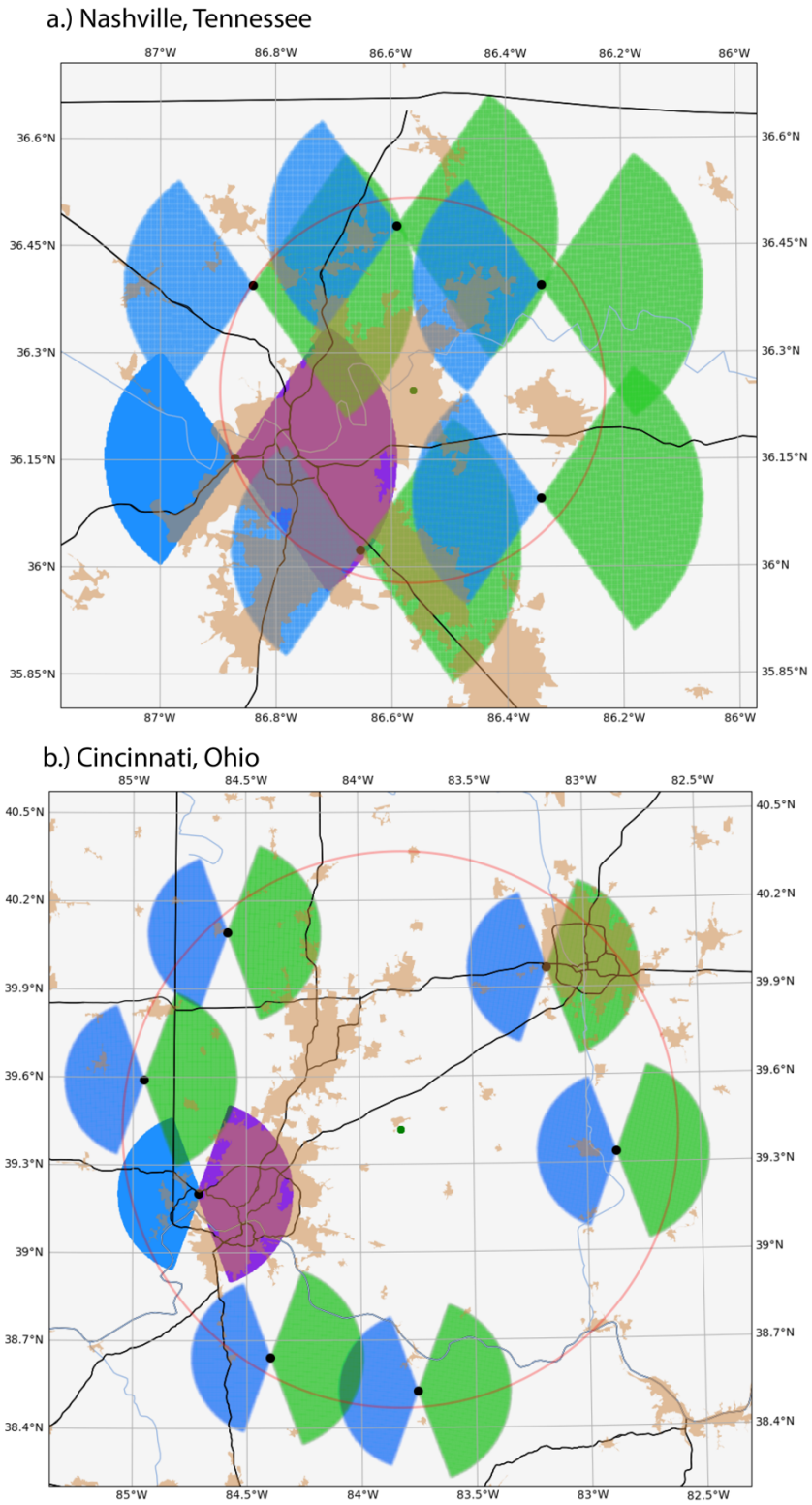

Figure 9. Same as Fig. 2, except for a) Nashville, Tennessee and b) Cincinnati, Ohio. The green dot in a) indicates the KOHX radar while the green dot in b) indicates the KILN radar. In b) a sixth comparison site is included (located at 39.9697º, -83.1691º) that overlaps the urbanized area of Columbus, Ohio.

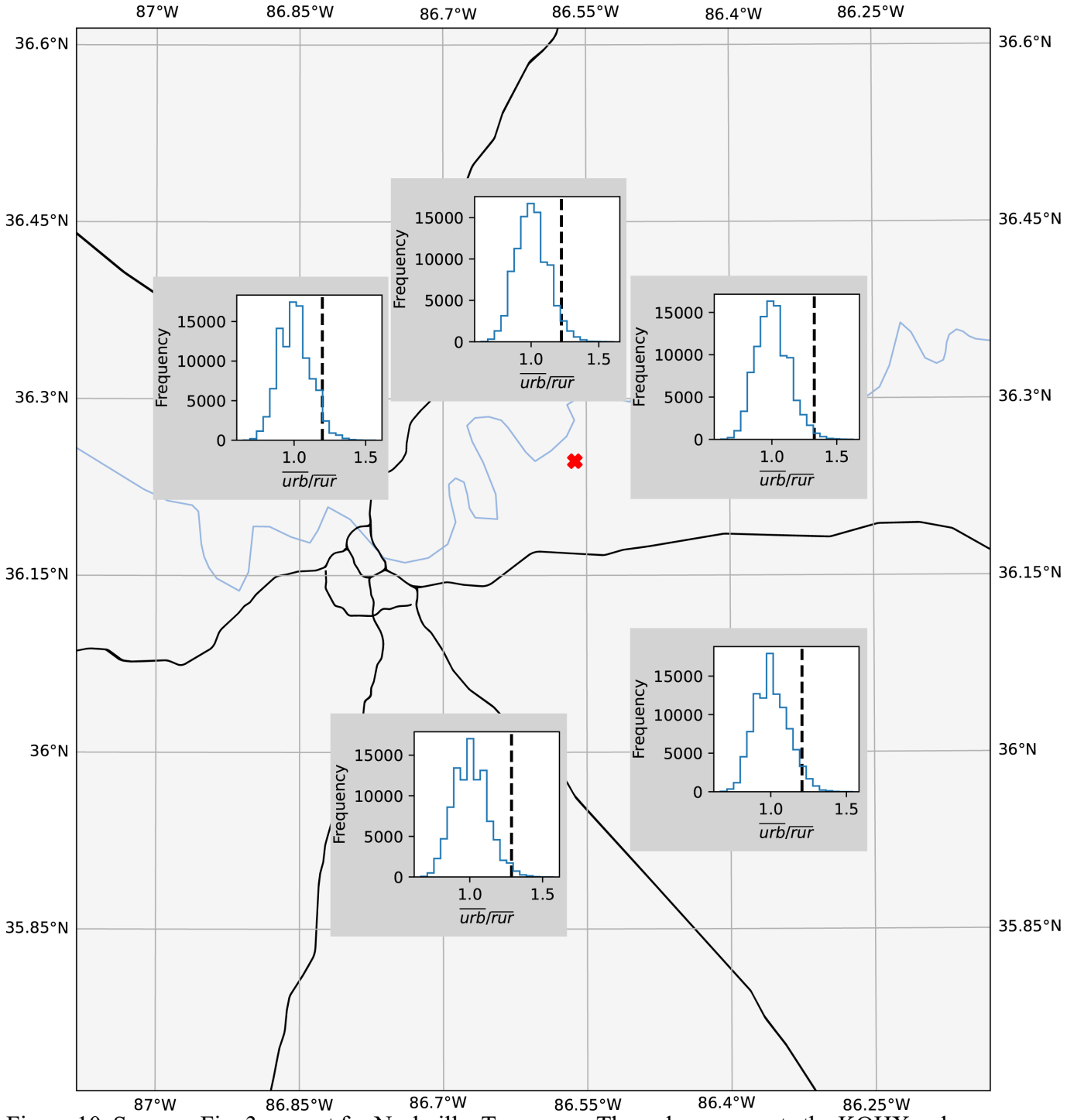

Figure 10. Same as Fig. 3, except for Nashville, Tennessee. The red x represents the KOHX radar.

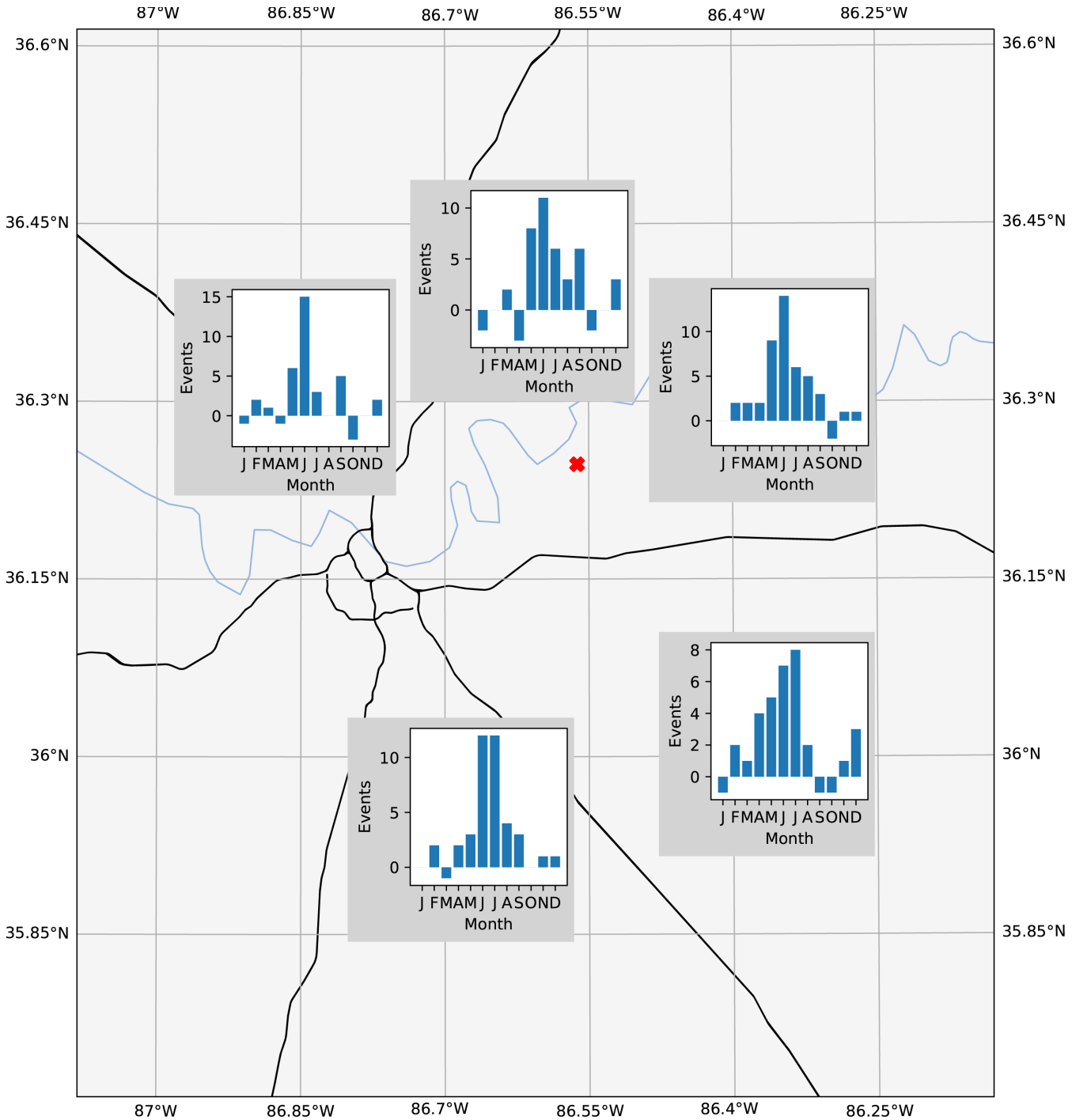

Figure 11. Same as Fig. 4, except for Nashville, Tennessee. The red x represents the KOHX radar.

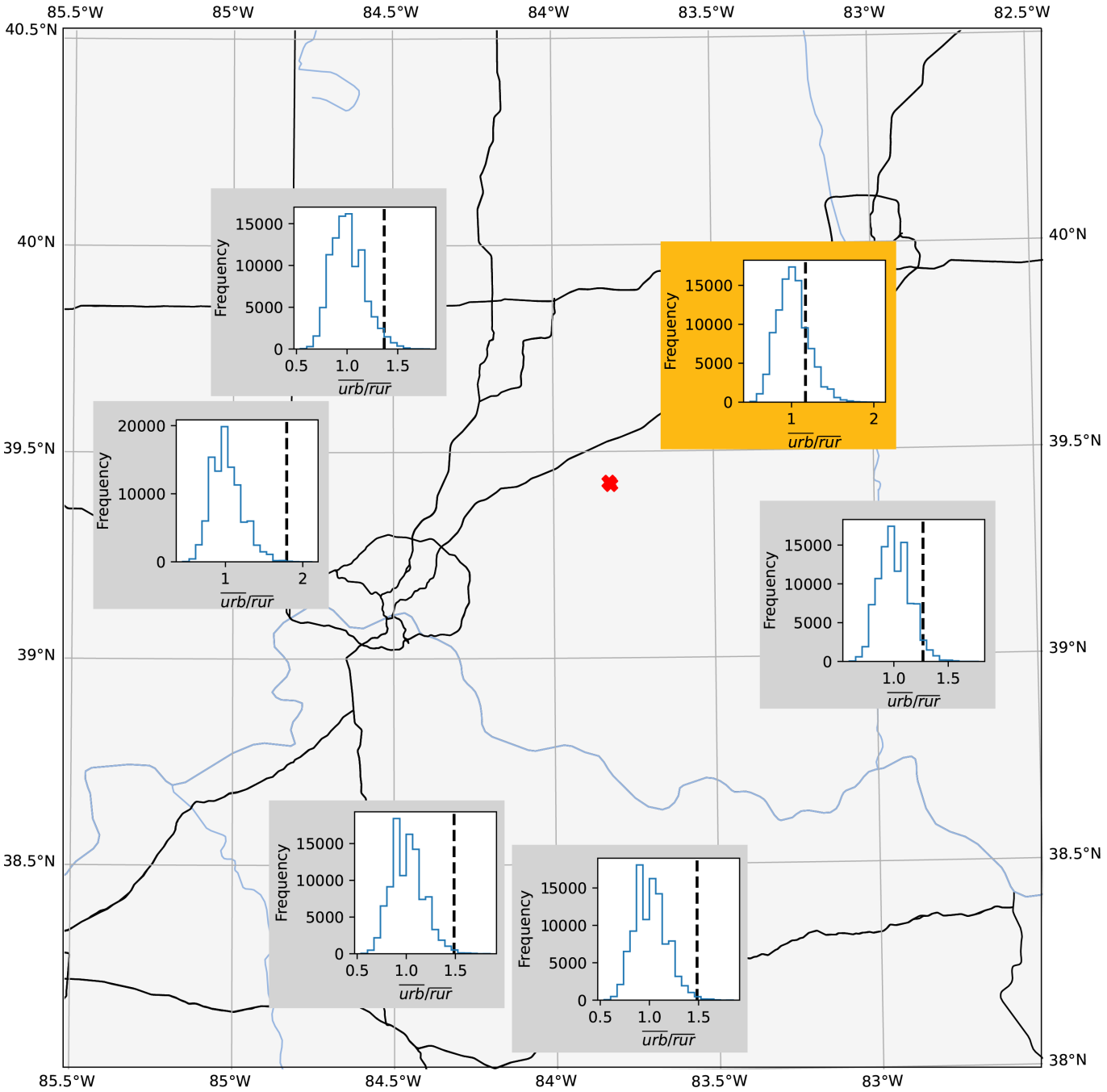

Figure 12. Same as Fig. 3, except for Cincinnati, Ohio. The red x represents the KILN radar. The graph outlined in orange represents the comparison location overlapping Columbus, Ohio.

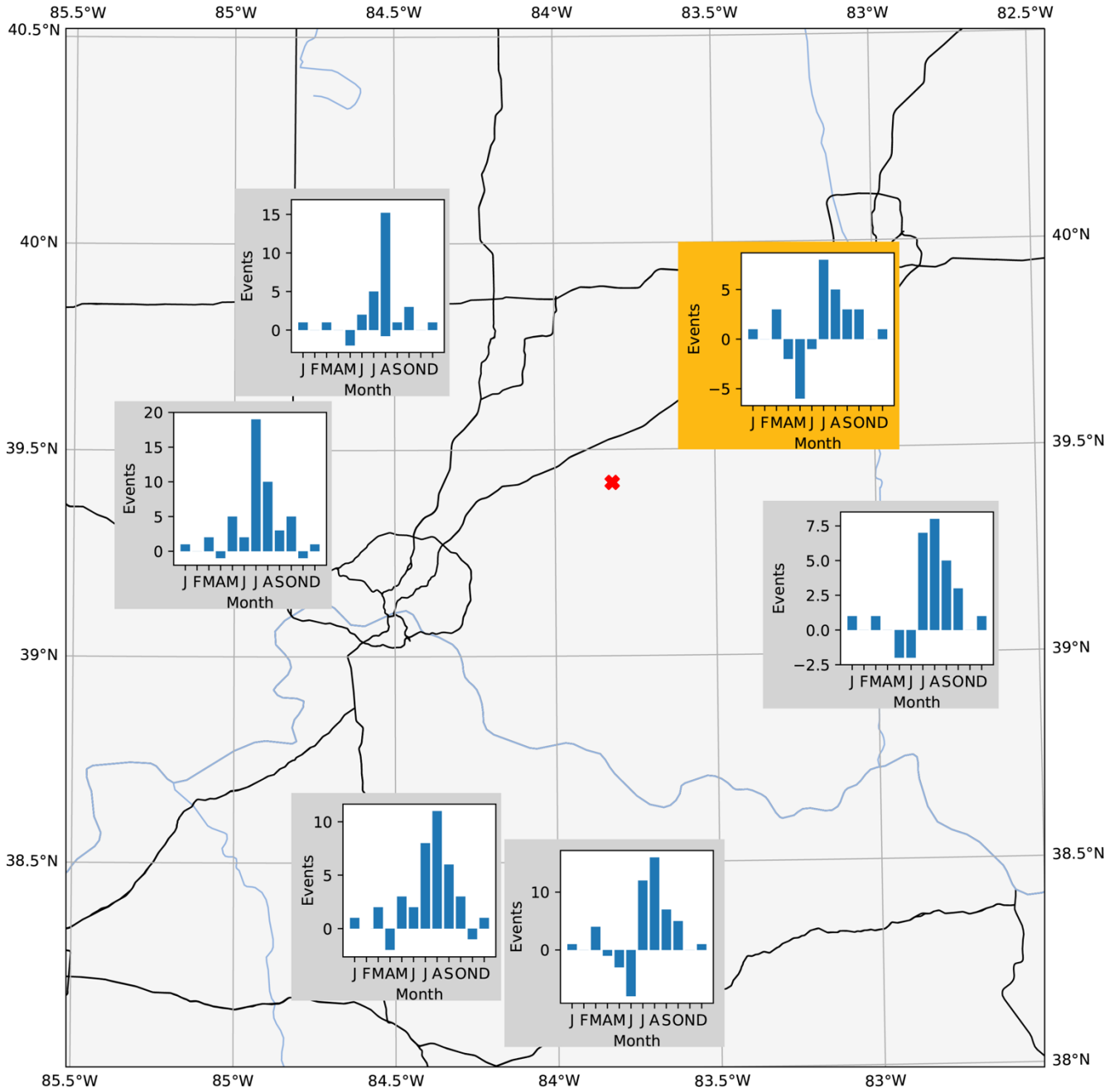

Figure 13. Same as Fig. 4, except for Cincinnati, Ohio. The red x represents the KILN radar. The graph outlined in orange is the same as in Fig. 12.

a.) 2019-07-10 18:00 UTC

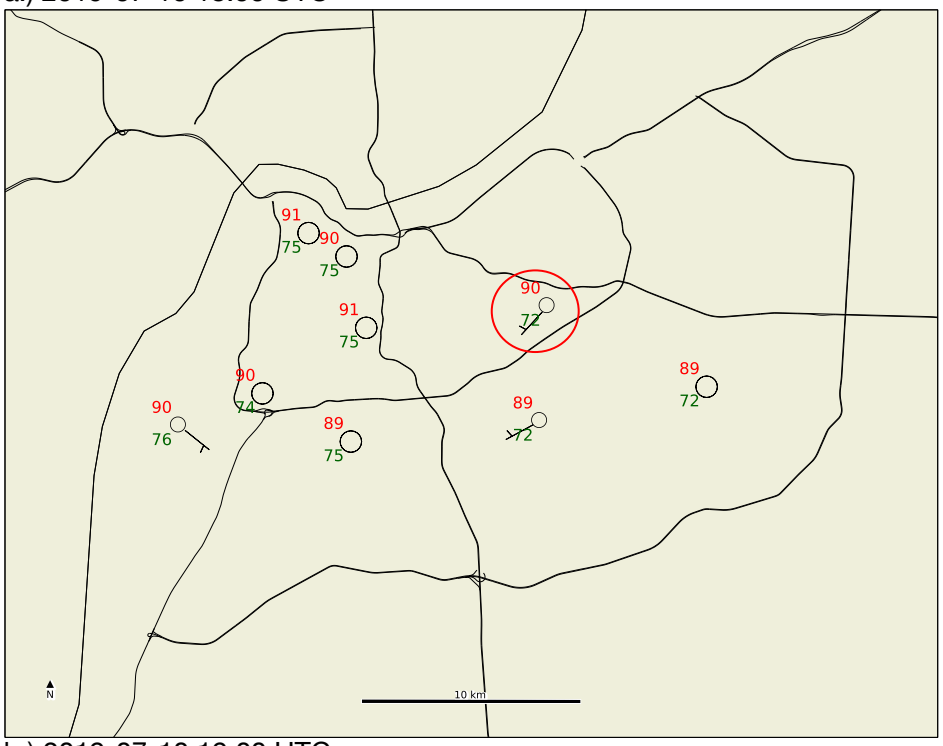

b.) 2019-07-10 19:00 UTC

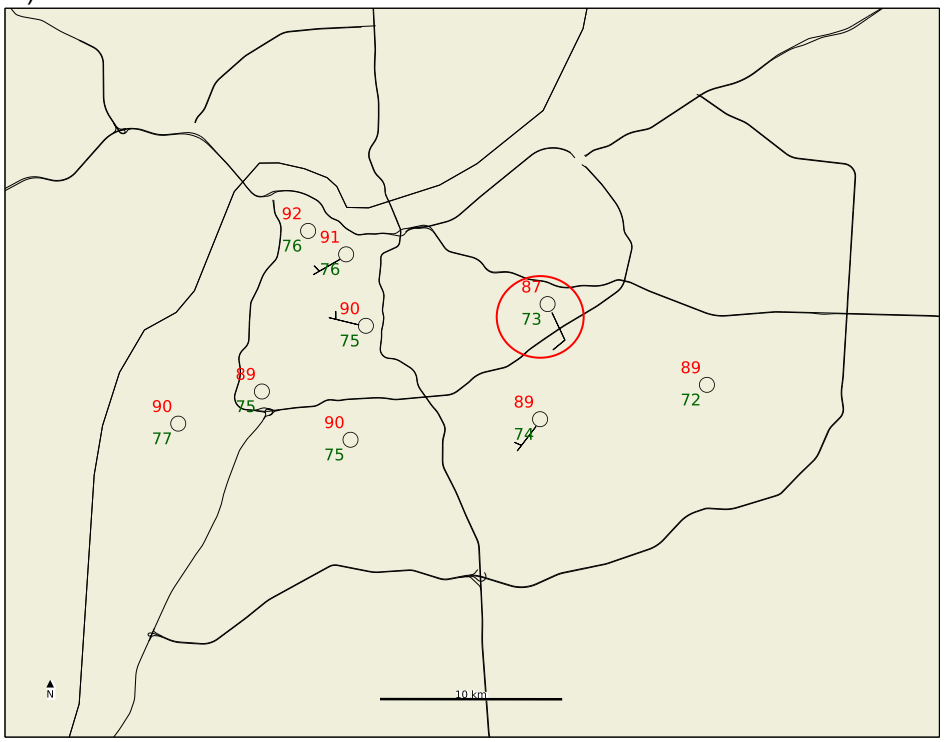

Figure 14. Station plots from surface observation stations around Louisville, Kentucky from a) 18 UTC on 10 July 2019 and b) 19 UTC on 10 July 2019. The Bowman Field station is circled in red. Wind observations at this station are taken at the standard 10 m level, while wind measurements from the other stations are from approximately 3 m agl.